Korean J. Chem. Eng., **26**(3), 711-718 (2009)

Effects of Cu_xTiO_y nanometer particles on biological toxicity during zebrafish embryogenesis

Min-Kyeong Yeo* and Misook Kang,†**

*Department of Environmental Science and Engineering, KyungHee University, Yongin, Gyeonggi 449-701, Korea
**Department of Chemistry, College of Science, Yeungnam University,
214-1 Daedong, Gyeongsan, Gyeongbuk 712-749, Korea
(*Received 2 September 2008 • accepted 4 December 2008*)

Abstract−This study investigated the toxicity of Cu (1, 10, 15, and 25 mol%) loaded TiO_2 and pure TiO_2 nanometer-sized photocatalysts during the development of zebrafish embryogenesis. The hatch rate decreased in the Cu_xTiO_y nanoparticles exposed groups (10, 20 ppt) compared to pure TiO_2 nano-particles (10, 20 ppt) exposed or control groups. These Cu_xTiO_y and TiO_2 nanoparticles led to developing mutated embryos with abnormal notochord formation, no tail, damaged eyes and abnormal heart development. Exposure to Cu_xTiO_y and pure TiO_2 nanoparticles led to glutathione increase, catalase activity increase, GST increase and GSR increase than control. Penetration of the Cu_xTiO_y and pure TiO_2 nanoparticles to the embryo was also tested. It was observed that Cu_xTiO_y and pure TiO_2 nanoparticles penetrated into cells. Moreover Cu_xTiO_y penetrated into the skin, nerve and yolk sac epithelium cells on the zebrafish larvae as aggregated particles, which may induce the direct interaction between nanoparticles and cell to cause adverse biological responses. As a result, the Cu-loaded TiO_2 nanoparticles had the toxicity of zebrafish embryo and larvae in the water environment.

Key words: Cu Loaded TiO_2 (Cu_xTiO_y), Nanoparticles, Oxidative Stress, Zebrafish Embryo

INTRODUCTION

Recently, numerous works have been done to display photocatalytic activity due to its promising performance in degrading various organic and inorganic environmental pollutants [1,2]. It has been reported that the addition of Pt [3], Cr^{3+} [4], Cu^{2+} [5], Fe^{3+} [6] and other cations [7] into anatase titania can improve its photoactivity. Among them, the Cu-doped TiO_2 system is considered as a potential candidate for photocatalyst, and it has been reported that the photocatalyst improved with optimal Cu content [8]. In particular, the technology for generating hydrogen by the splitting of water using a Cu-doped TiO_2 photocatalyst has attracted much attention. The production of H_2 from methanol/water photodecomposition was greater over the Cu_xTiO_y nanosized photocatalysts than over the pure nanometer-sized TiO_2 [8]. Based on the result, a model was developed to explain the effect of the CuO component existing on the external surface of TiO_2 for high H_2 production from the methanol/water photodecomposition reaction. If the CuO component exists on the external surface of TiO_2, it will be reduced to Cu_2O or Cu by attracting the excited electrons from the valence band of TiO_2. Since the reduction potential of CuO (E_0=0.157 or 0.340) is greater than that of pure TiO_2, the reduction of Cu^{2+} to Cu^{1+} or Cu^0 is possible. Consequently, the recombination of an electron and a hole is difficult, as the CuO component captures electrons, increasing the number of holes over the valence band, allowing methanol decomposition to continue.

However nanosized pure TiO_2 has been the focus of much research, such as in environmental toxicity [9-11]. Many studies have documented the phototoxic and photo-genotoxic effects of TiO_2 (both normal and nanometer-sized) [12-16], and consequently its properties as a photo-catalytic compound have been applied to waste water disinfection [17] and photodynamic therapy of certain cancers [18]. Additionally, anatase (10 and 20 nm) TiO_2 particles, in the absence of photo-activation, induced oxidative DNA damage, lipid peroxidation, micronuclei formation, and increased hydrogen peroxide and nitric oxide production in a human bronchial epithelial cell line [9]. While there is ample evidence of the formation of reactive oxygen species (ROS) when TiO_2 is exposed to UV light [19-21], there is disagreement as to the exact nature of the species produced and their involvement in cell death. Possible ROS that could be formed are hydroxyl radicals (•OH), superoxide radical anions (O^{2-}), hydrogen peroxide (H_2O_2) and singlet oxygen. These species can be identified by means of electron spin resonance (ESR), by using the technique of spin trapping. Additionally, Long et al. [22] found that TiO_2 causes oxidative stress in brain microglia cells under in vitro conditions. Moreover, CuO in wood preservation and antimicrobial textiles [23,24] has been used, and CuO nanoparticle was evaluated for toxicity to several bacteria [25]. Given that nanotechnology industries plan large scale production, it is inevitable that these products and their by-products will accumulate in the aquatic environment [26,27], and their potential genotoxic effects could have short and long-term consequences for the biota [28]. However, there are few researches about toxicity of the addition of cation into anatase TiO_2.

In the present work, we evaluated the toxic effect of the Cu (1, 10, 15, and 25 mol%) loaded TiO_2 (Cu_xTiO_y) and pure TiO_2 nanoparticles using zebrafish embryos. Furthermore, hatching rate, intracellular GSH (total glutathione) levels, and antioxidative enzymes (glutathione S-transferase; GST, glutathione reductase; GSR, and

†To whom correspondence should be addressed.
E-mail: mskang@ynu.ac.kr

catalase) activities as markers of oxidative stress by OH- radical were also investigated. Additionally, penetration of Cu_xTiO_y and pure TiO_2 was observed by TEM.

EXPERIMENTAL

1. Preparation of TiO_2 and Cu_xTiO_y Samples

TiO_2 and Cu_xTiO_y nanometer-sized samples were donated by Kang et al. working [8] for Young Nam University, Korea. An HRTEM (high resolution transmission electron microscope, JEOL, Japan), with an accelerating voltage of 300 kV, was used to study these structures and morphologies of TiO_2 and Cu_xTiO_y nanosized photocatalysts. For TEM imaging, the sample was placed on copper grids. The TiO_2 and Cu_xTiO_y powders were subjected to XRD (model PW 1830; Philips, Amsterdam, The Netherlands), with nickel-filtered CuKα radiation (30 kV, 30 mA) at 2θ angles from 5° to 70°, with a scan speed of 10°/min and time constant of 1 s. The sizes and shapes of the TiO_2 and Cu_xTiO_y particles were observed by scanning electron microscope (SEM, model JEOL-JSM35CF; Tokyo, Japan), with the power set to 15 kV.

2. Experimental Animals

Zebrafish (Danio rerio, wild-type) ~7-8 months old and bred in our laboratory were used. The zebrafish breeding conditions, development stage, morphology, and hatching rate were examined according to previous research [29]. A 60 L glass water tank contained the aquatic environment filtered by a carbon filter. The water temperature was maintained at 28±1 °C, and the light/dark cycle was 14 h. Adult fish were fed blood worms, dry flake food, and brine shrimp. Eggs were laid and fertilized within 1 h of the beginning of the light cycle, which provided large populations of synchronously developing embryos. The embryos were collected, pooled, and rinsed several times. Embryonic staging was carried out according to the standardized staging series set forth by Kimmel et al. [30]. The embryos were immersed in exposure or vehicle control solutions beginning at the 64- to 256-cell stages, and 2.5 hour post-fertilization (hpf). Dead embryos were removed to avoid contaminating the test solutions. Embryos were observed with a microscope (Olympus, SZ61, Japan) to determine morphological effects.

3. Chemical Exposure During Development Stage

Cu_xTiO_y and TiO_2 nanoparticles which were suspended in cityl water were allowed to stand for 24 hours to evaporate chlorine, as recommended [29]. The final nanoparticles' (TiO_2, Cu_xTiO_y) exposure concentrations were 10 and 20 ppt in each group. Each group of embryos was placed in 1-L glass beakers and maintained in a carbon-filtrated water system at 28±1 °C. Each group contained 300 variable embryos. Embryos were randomly divided into the following groups: Group 1 was the general control group; Group 2: TiO_2 and Group 3 embryos were exposed to Cu (1, 10, 15, and 25 mol%) loaded TiO_2 nanoparticles. Embryos were observed at 2, 5, 8, 22, 27, 32, 48, 52, and 72 hpf, which are time points based on known developmental stages [30]. Dead embryos were removed during development. We calculated the hatching rates at 72 hpf for

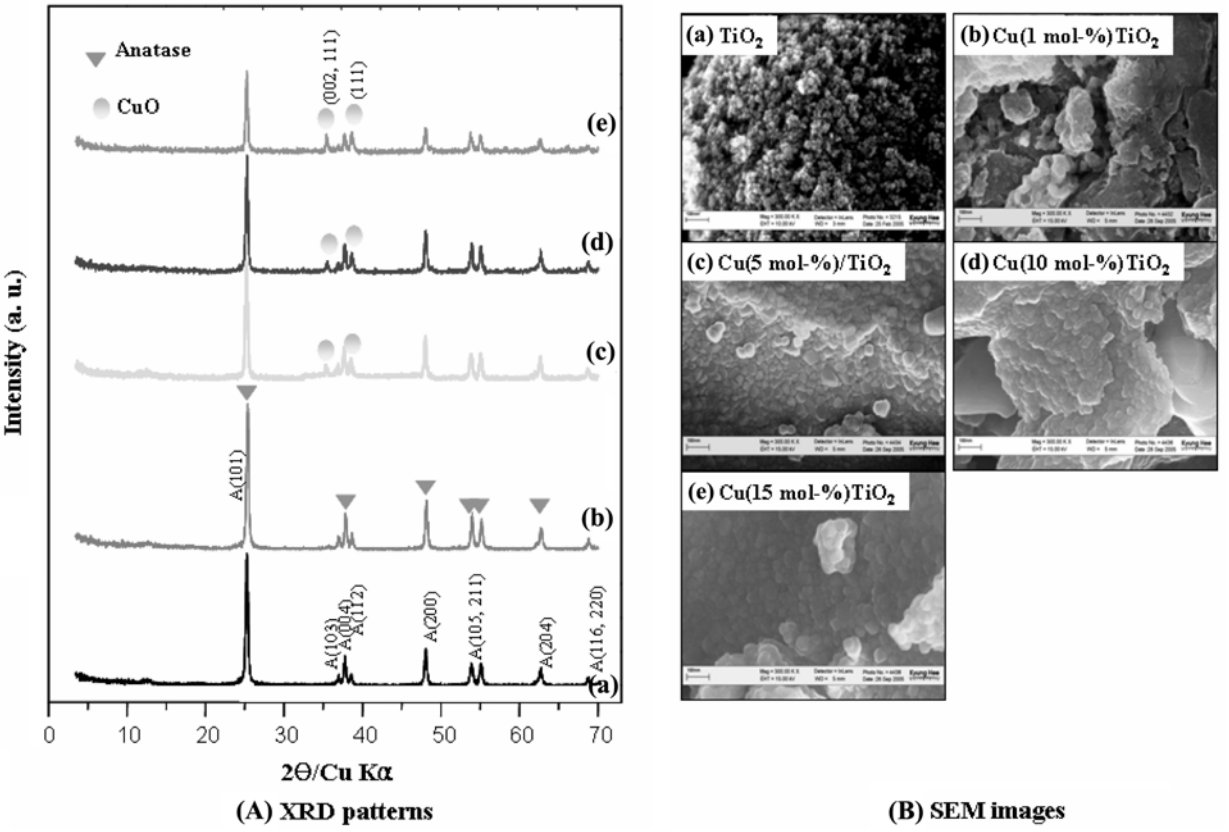

Fig. 1. The XRD patterns and SEM images of TiO_2 and the Cu (1, 10, 15, and 25 mol%) loaded TiO_2, Cu_xTiO_y after treatment at 500 °C: (a) TiO_2 treated at 500 °C, (b) 1 mol% Cu_xTiO_y treated at 500 °C, (c) 5 mol% Cu_xTiO_y treated at 500 °C, (d) 10 mol% Cu_xTiO_y treated at 500 °C, and (e) 15 mol% Cu_xTiO_y treated at 500 °C.

the experimental and control groups.

4. Anti-oxidant Enzyme Activity Assays

Assay for glutathione (GSH) content: The level of total cellular GSH was measured according to the fluorometric method described previously [31]. Briefly, 10 µl of the sample was incubated with 12.5 µl of 25% metaphosphoric acid, and 37 µl of 0.1 M sodium phosphate buffer containing 5 mM EDTA, pH 8.0 at 4 ºC for 10 min. The samples were centrifuged at 13,000 g for 5 min at 4 ºC. The resulting supernatant (10 µl) was incubated with 0.1 ml of o-phthalaldehyde solution (0.1% in methanol) and 1.89 ml of the above phosphate buffer for 15 min at room temperature. Fluorescence intensity was then measured by using a Perkin-Elmer fluorometer (LS50B) at an excitation wavelength of 350 nm and an emission wavelength of 420 nm. GSH content was calculated with a concurrently run GSH (Sigma) standard curve, and expressed as nmol of GSH per mg of total cellular or mitochondrial protein.

Assay for glutathione reductase (GSR) activity: The method described before [32] was followed to measure the activity of total cellular and mitochondrial GSR in a final reaction volume of 0.6 ml. Briefly, to an assay cuvettes containing 0.46 ml of 50 mM potassium phosphate buffer (pH 7.0) and 1 mM EDTA, 20 µl of sample and 60 µl of 20 mM oxidized form of glutathione (GSH) were added. The cuvettes were pre-warmed at 37 ºC for 3 min. The reaction was started by adding 60 µl of 1.5 mM NADPH (prepared in 0.1% $NaHCO_3$). The subsequent consumption of NADPH was monitored at 340 nm, 37 ºC for 5 min. GSR activity was calculated by using the extinction coefficient of 6.22 mM^{-1} cm^{-1}, and expressed as nmol of NADPH consumed per min per mg of total cellular protein.

Assay for glutathione S-transferase (GST) activity: Cellular GST activity was measured according to the method of Habig et al. [33] using 1-chloro-2,4-dinitrobenzene (CDNB) as a substrate in a final reaction volume of 0.6 ml. Briefly, the reaction mix contained 1 mM GSH, 1 mM CDNB and 3 mg/ml of bovine serum albumin in 0.1 M sodium phosphate buffer, pH 6.5. 0.59 ml of the above reaction mix was added to each cuvette. The reaction was started by adding 10 µl of sample, and the rate of formation of CDNB-GSH conjugate was monitored at 340 nm, 25 ºC for 5 min. GST activity was calculated from the extinction coefficient of 9.6 mM^{-1} cm^{-1}, and expressed as nmol of CDNB-GSH conjugate formed per min per mg of cellular protein.

Catalase activity: Samples were taken from each group and treated as described below. Five zebrafish larvae were homogenized in 1 ml phosphate buffer (0.1 M, pH 7.3). The homogenate was centrifuged at 9,000 x g for 5 min at 4 ºC. The supernatant, containing enzyme, was reacted with H_2O_2 for 1 min at 37 ºC. The reaction was stopped with 32.4 mmol/L ammonium molybdate, and enzyme activity meas-

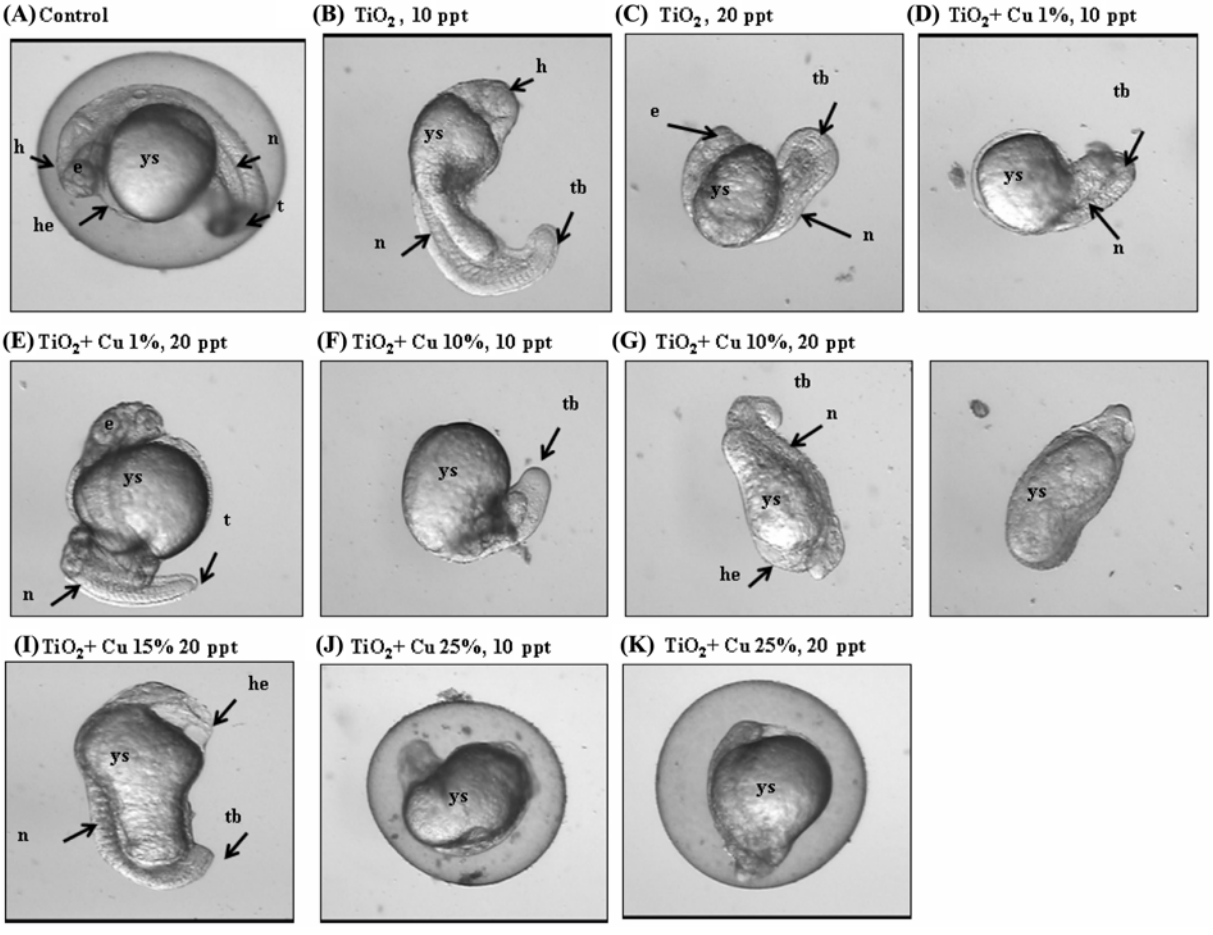

Fig. 2. The effects of the Cu (1, 10, 15, and 25 mol%) loaded TiO_2 and pure TiO_2 nanosized photocatalysts on the development of zebrafish. Embryos were exposed to pure TiO_2 or Cu_xTiO_y in 10 ppt and 20 ppt. These images show exposed zebrafish at 20 hpf. Abbreviations: e, eye; h, head; he, heart; n, notochord; t, tail; t b, tail bud; ys, yolk sac.

ured at 405 nm with a UV-Vis spectrophotometer (UV-1601PC, Shimadzu, Japan).

5. Histological Preparation, Transmission Electron Microscopy (TEM), and Statistical Analyses

Tissue was fixed at 4 ºC in 2% glutaraldehyde in sodium phosphate buffer, post fixed in 1% osmium tetroxide, dehydrated through graded ethanol solutions and then embedded in Embed 812-Araldite 502 resin (EMS). For transmission electron microscopy, ultra-thin sections (from 60 to 70 nm of depth) were mounted on copper grids, and then stained in lead citrate and uranyl acetate solutions for examination. The sample was observed by using the field emission transmission electron microscope (FE TEM, H-7600, operated at 80 kV, Hitachi, Japan). All graphs and statistical analyses were performed with Excel 2003 (Microsoft, USA). All data were collected for groups consisting of 300 embryos. Each experiment was conducted in triplicate. Data were analyzed by using a paired one-tailed Student's t-test to determine the lowest statistically significant concentration relative to an unexposed baseline control.

RESULTS AND DISCUSSION

1. Characteristics of Cu Loaded TiO_2 (Cu_xTiO_y) and Pure TiO_2 Nanosized Photocatalysts

The XRD patterns (A) and SEM images (B) of Cu (1, 10, 15, and 25 mol%) loaded TiO_2 and pure TiO_2 nanosized photocatalysts are discussed in Fig. 1. The diffraction peaks for the anatase phases are labeled "A," with the corresponding diffraction planes given in parentheses. Both TiO_2 and Cu_xTiO_y showed well-developed anatase structures after treatment at 500 ºC. The peaks at 2θ=35.50º and 38.73º, which were assigned to CuO (002 or 111) and CuO (111), respectively, were seen for the photocatalysts with above 5 mol% Cu_xTiO_y, and the intensities increased with increasing amount of loaded Cu. These results indicate that the Cu components exist on the external surface of TiO_2, and are unlikely to be incorporated into the framework of the anatase structure. Fig. 1 B shows SEM photographs of the TiO_2 and Cu_xTiO_y particles. The photocatalysts consisted of relatively irregular, spherical particles, 30-50 nm in size. For Cu_xTiO_y, the particles were larger than those of pure TiO_2, which is related to a sintering effect due to the increased agglomeration between CuO and TiO_2 particles. The Cu compositions on the Cu/TiO_2 anatase structure were estimated by using energy dispersive X-ray (EDAX) analysis; the ratios of Cu/Ti were 0.026, 0.023, 0.093 and 0.275 in 1, 5, 10 and 15 mol% Cu_xTiO_y, respectively. Consequently, pure TiO_2 nanosized photocatalysts could increase the photocatalysis effect; moreover, the Cu_xTiO_y results in an increased photocatalysis effect than pure TiO_2.

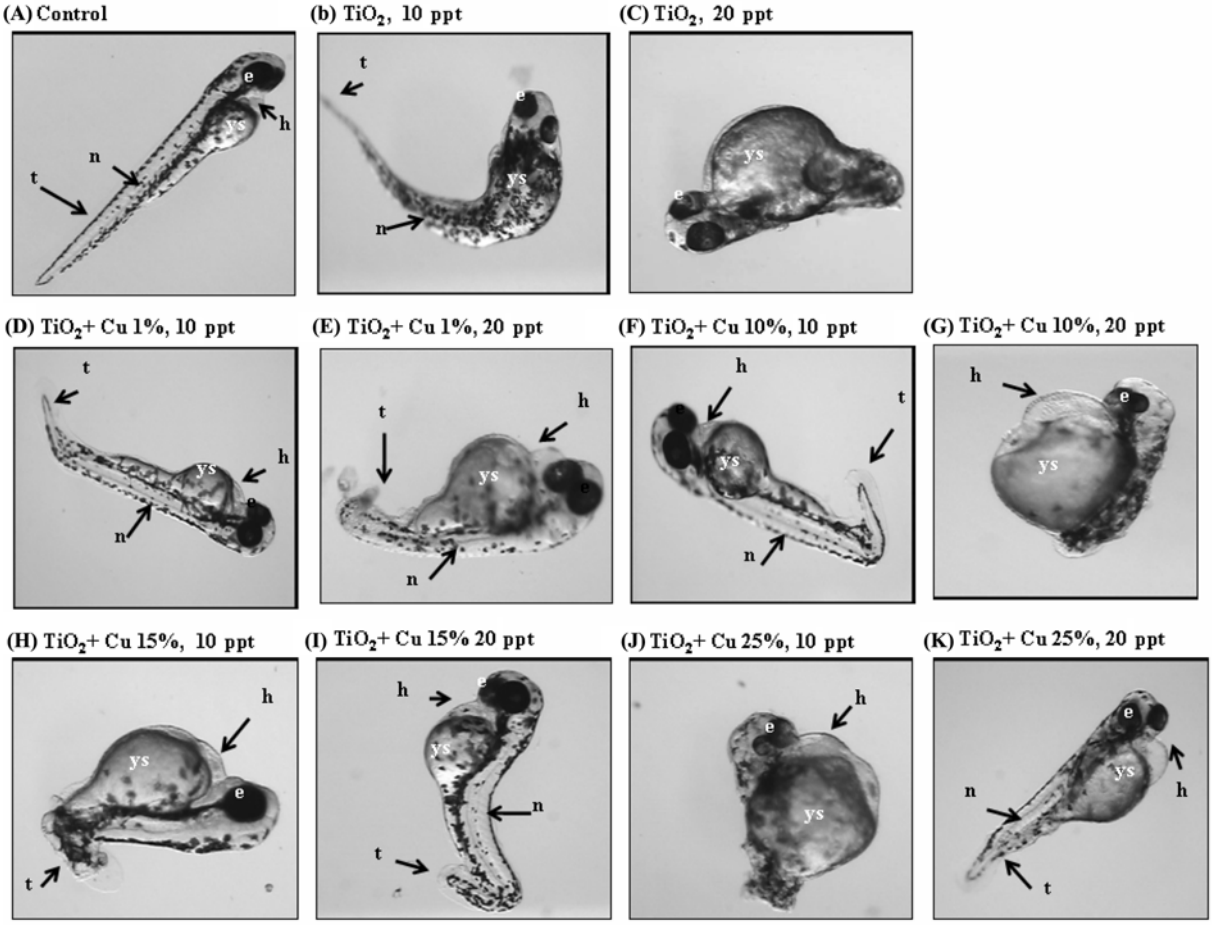

Fig. 3. The effects of the Cu (1, 10, 15, and 25 mol%) loaded TiO_2 and pure TiO_2 nanosized photocatalysts on the development of zebrafish. Embryos were exposed to pure TiO_2 or Cu loaded TiO_2 in 10 ppt and 20 ppt. These images show exposed zebrafish at 48 hpf. Abbreviations: e, eye; h, head; he, heart; n, notochord; t, tail; t b, tail bud; ys, yolk sac.

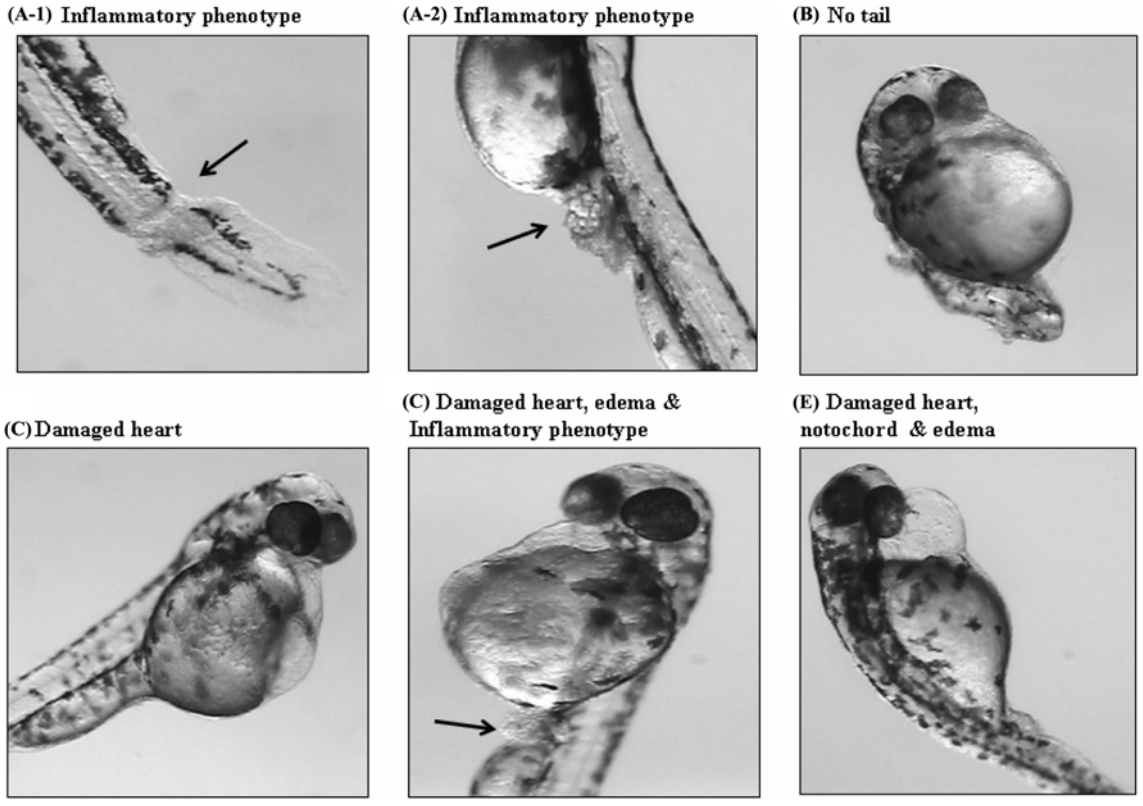

Fig. 4. The properties of abnormal morphologies are among surviving embryos.

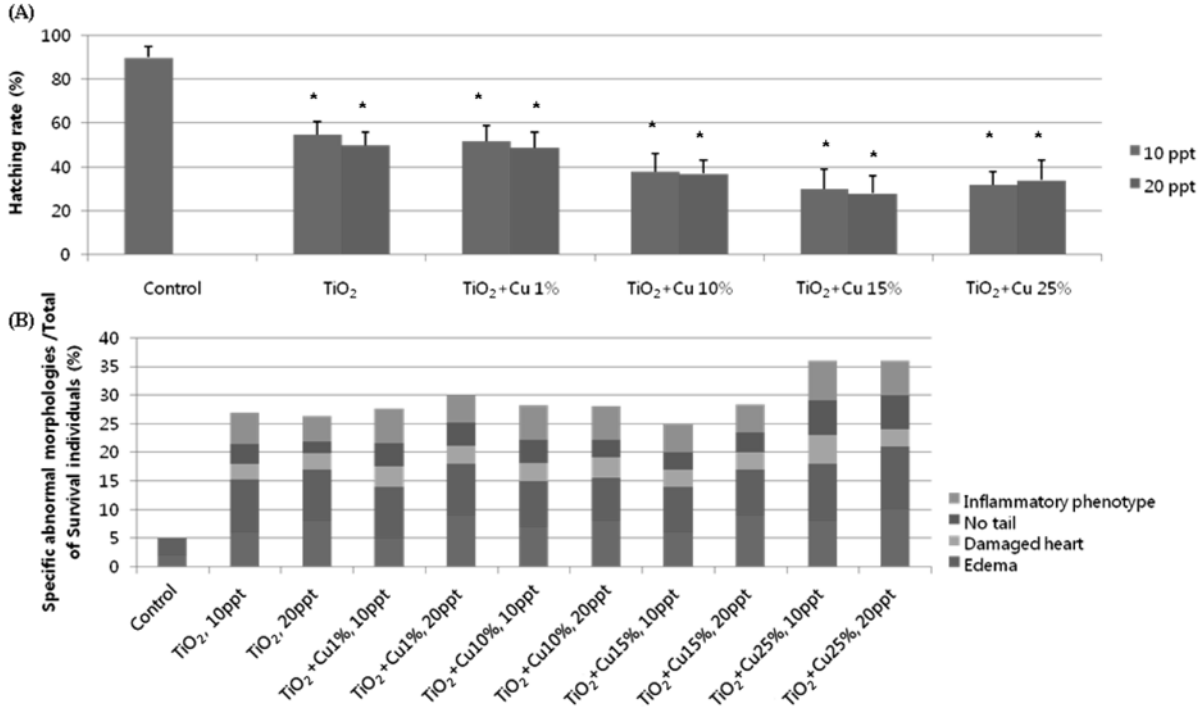

Fig. 5. The effects of nanometer sized Cu loaded TiO_2 on the hatching rate (A) and rates of specific abnormal morphologies among surviving embryos (B). The hatching rate decreased in groups exposed to the Cu (1, 10, 15, and 25 mol%) loaded TiO_2 and pure TiO_2 nanosized photocatalysts (10 ppt, 20 ppt) compared to the control group. In particular, hatching rate in the Cu_xTiO_y and pure TiO_2 nanosized photocatalysts (10 ppt, 20 ppt) exposed groups are significantly decreased than that in the control group. Rates of specific abnormal morphologies among surviving embryos in the Cu_xTiO_y and pure TiO_2 nanosized photocatalysts exposed groups are also shown to be increased. The properties of abnormal morphologies are inflammatory phenotype, no tail, damaged heart and edema.

2. The Effects of Nanometer-sized Cu Loaded TiO_2 on the Development Stages of Zebrafish

The effects of TiO_2 and Cu_xTiO_y nanometer-sized photocatalysts on the embryogenesis zebrafish are shown in Figs. 2 and 3. The embryos were evaluated 24 hpf (hours post fertilization) in Fig. 2. In the groups exposed to the Cu_xTiO_y and pure TiO_2 nanosized photocatalysts very seriously injured larvae were detected, and many had abnormal notochord development, which were loss or curved in both (10 and 20 ppt) groups. Some of them lacked head development (Figs. 2 D, F, H and I). The embryos were evaluated 48 hpf during the Long-pec stage in Fig. 3. In the control group, black colored eyes, vacuolated differentiating cells in the notochord, and a yolk sack approximately equal to the volume of the head were observed. However, for the groups exposed to the Cu_xTiO_y and pure TiO_2 nanosized photocatalysts very seriously injured larvae were detected, and many had abnormal notochord development, which were very short and curved in both (10 and 20 ppt) groups. Furthermore, the tails were not developed in some larvae (Fig. 3 C, G, H, and J). At this stage, the size of the yolk sack was approximately equal to the head, but the size of the head was smaller than the yolk sack in fish with damaged tail and heart. On the basis of these results, it is suggested that nanosized Cu have an effect in the zebrafish larvae, because Cu can act as Na analogues and competitors in gill transport systems, and out-compete Na, thereby blocking transport systems [34] and [35]. Moreover, ion regulation is initially exclusively transcutaneous in developing fish. As in the gill of adult fish, mitochondria-rich cells (MRCs) appear to be the primary cell type involved. Briefly, mitochondria-rich cells first appear in the skin and yolksac epithelium of developing fish during late gastrulating or early organogenesis [36]. In addition, the higher toxicity of nano CuO (metal basis) was probably due to bioavailability of Cu ions as Cu^{2+} was toxic to bacteria [25]. From this result, it is suggested that nanometer-sized Cu_xTiO_y could be for use in antibacterial applications. However, nanometer-sized Cu_xTiO_y could enter a cell and affect the ion regulation in the skin and yolksac epithelium of development zebrafish. It is the cause of lethal injury in zebrafish. The size relationship observed in this study has been reported by several other researchers [37-39]. In this study, exposure to the Cu_xTiO_y and pure TiO_2 nanosized photocatalysts caused zebrafish embryos to develop abnormally (Figs. 2, 3 and 4), which may be due to nanometer-sized CuO and TiO_2 entering the embryo membrane.

The specific abnormal morphologies in the embryogenesis zebrafish are shown in detail; Figs. 4 and 5 denote the accumulation of specific abnormal morphologies/total numbers of surviving individuals (%). Almost all the individuals in the Cu_xTiO_y and pure TiO_2 nanosized photocatalysts (10 ppt and 20 ppt) exposed groups had ab-

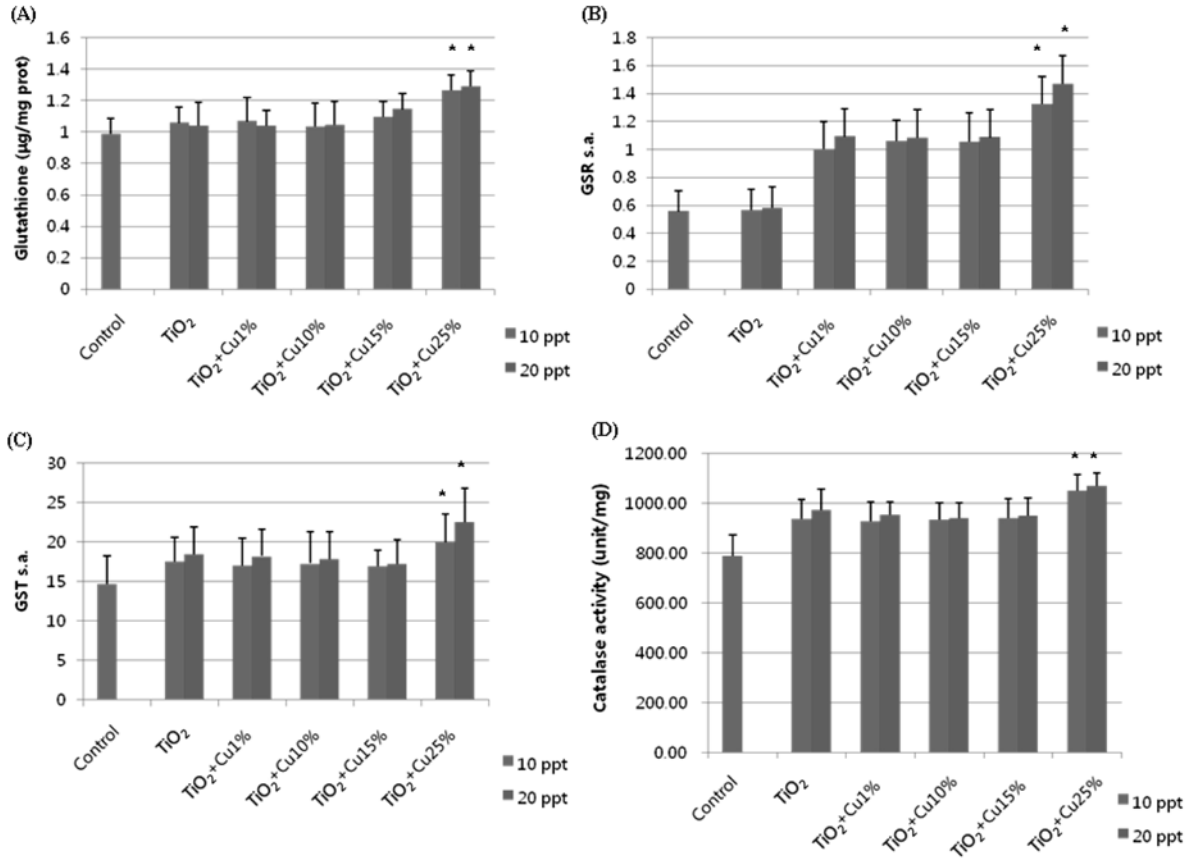

Fig. 6. The effects of the Cu (1, 10, 15, and 25 mol%) loaded TiO_2 and pure TiO_2 nanosized photocatalysts on the glutathion (A) and antioxidative enzymes activities; GSR (B), GST (C) and catalase (D). The amount of glutathione and antioxidative enzymes activities in the Cu_xTiO_y and pure TiO_2 nanosized photocatalysts exposed groups are also shown to be increased. In particular, the amount of glutathione and antioxidative enzymes activities in the Cu 25 mol% loaded TiO_2 (TiO_2+Cu 25%, 10 ppt and 20 ppt) exposed groups are significantly greater than that in the control group.

normal properties, including inplammatory phenotype, edema and abnormal notochords. Especially, there were increased edema and inflammatory phenotype in the Cu 25 mol% loaded TiO_2 10 and 20 ppt nanosized photocatalysts exposed group compared with those in the other exposed groups and control. The hatching rates were significantly decreased in both the Cu_xTiO_y and pure TiO_2 nanosized photocatalysts (10 ppt and 20 ppt) exposed groups compared to the control (Fig. 5A). Moreover, the glutathione, GSR, GST and catalase activities in the hatched larvae of both the treated groups were increased compared to the control, while that in the Cu 25 mol% loaded TiO_2 10 and 20 ppt nanosized photocatalysts exposed groups were significantly greater than in the control group (Fig. 6). The main mechanism of toxicity of nanosized particles is thought to be via oxidative stress [40] that damages lipids, carbohydrates, proteins and DNA [41]. Lipid peroxidation is considered most dangerous as leading to alterations in cell membrane properties, which in turn disrupts vital cellular functions [42]. OS-mediated toxicity has been shown for TiO_2 in in-vitro studies, including brain cells [43]. Near-UV-light potentiates the toxicity and genotoxicity of TiO_2 [44,45]. Xia et al. [46] have shown that the toxicity of nanoparticles might be predicted from their ROS generation capability in vitro.

Based on the results shown in Fig. 6, it is suggested that oxidative stress was induced by Cu-loaded TiO_2 nanosized photocatalysts in zebrafish embryogenesis. The glutathione, GSR, GST and catalase activities in the hatched larvae of both the treated groups were increased compared to the control, while that in the Cu 25 mol% loaded TiO_2 10 and 20 ppt nanosized photocatalysts exposed groups were significantly greater than in the control group (Fig. 6). This result was believed to be due to the free radicals produced, while it is the role of antioxidative enzymes to remove free radicals. The increased GSH, GSR, GST and catalase activities in Cu_xTiO_y or pure TiO_2 nanosized photocatalysts exposed groups are suggested

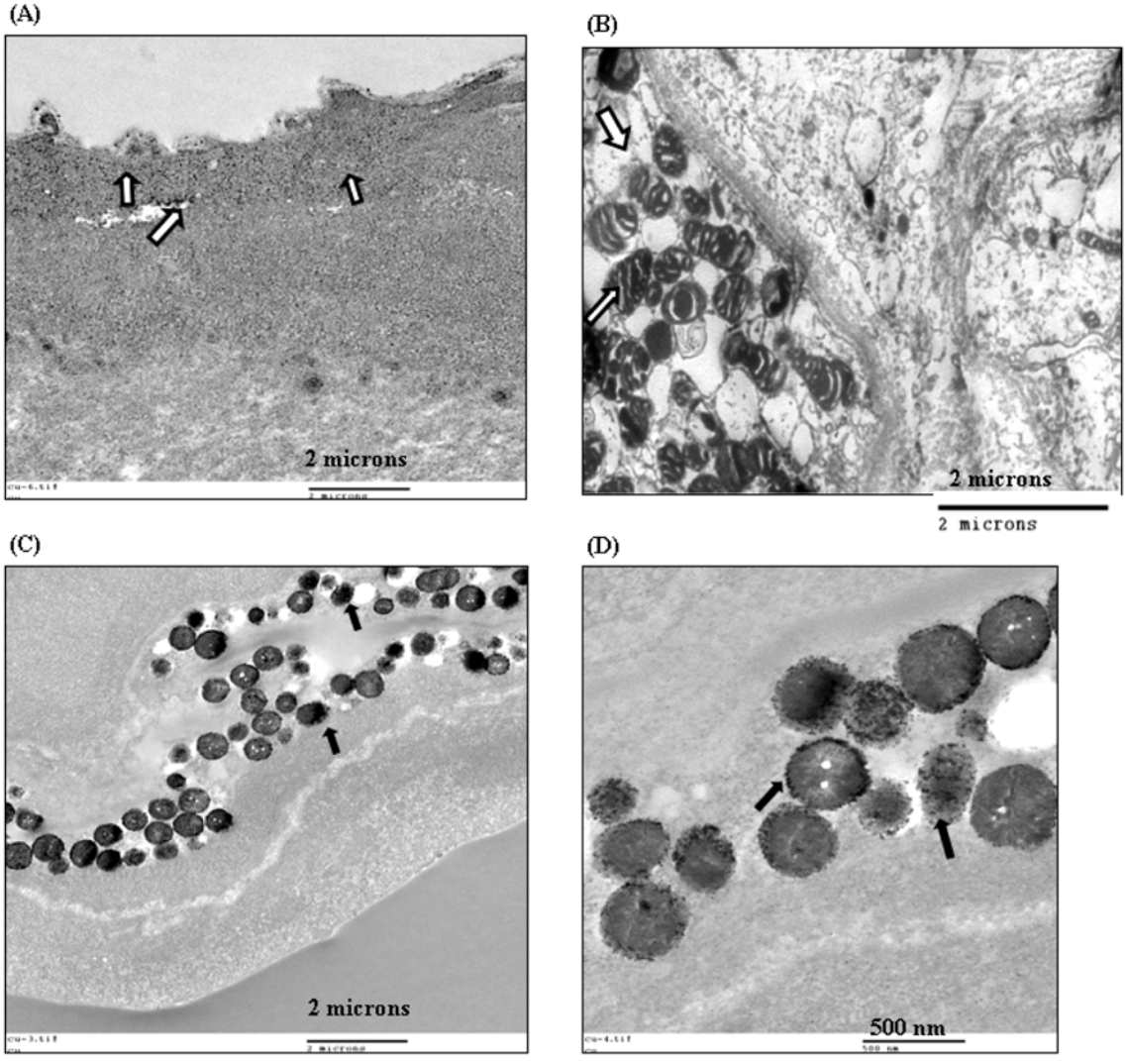

Fig. 7. TEM micrographs of TiO_2 and Cu_xTiO_y nanoparticle-treated larvae samples. Tissue specimens were fixed in TEM buffer, post-fixed in osmium tetroxide and uranyl acetate, embedded in an Epon-based resin, cut as 60- to 90-nm-thick sections. For details on sample preparation, refer to the Materials and Methods section. Selected micrographs show (A) skin of zebrafish larvae exposed with TiO_2 nanoparticles (white arrows; TiO_2 nanoparticles), and (B) nerve cells on Cu_xTiO_y nanoparticle-treated larvae (white arrows; nerve cells and penetrated nanoparticles) (C) yolksac epithelium cells on the zebrafish larvae as aggregated particles (black arrows; Cu_xTiO_y nanoparticle). (D) Cu_xTiO_y nanoparticles penetrated into epithelium cells and attached around vessels.

to be the result of cellular damage due to free radicals.

It was shown that Cu_xTiO_y and pure TiO_2 nanoparticles penetrated into cells (Fig. 7). Moreover Cu_xTiO_y penetrated into the skin, nerve and yolksac epithelium cells on the zebrafish larvae as aggregated particles. Based on the results, this may induce a direct interaction between nanoparticles and cells to cause adverse biological responses. In addition, it has also recently been reported that the MRCs on the skin of zebrafish larvae appear to be innervated, raising the possibility that ionoregulation may come under nervous control at an early age [47].

CONCLUSION

Based on current evidence, it would appear that except for the location (skin vs. gills), the basic physiology of ionoregulation is virtually identical in post-gastrula embryos and larvae. It suggests that the Cu-loaded TiO_2, Cu_xTiO_y could penetrate to the MRCs on the skin of zebrafish larvae and it could affect mitochondrial oxidative stress and lead to developmental injury.

ACKNOWLEGMENT

This work was supported by the National Center for Nanomaterials Technology through Yeungnam University in 2008.

REFERENCES

1. T. Sreethawong, Y. Suzuki and S. Yoshikawa, *Catal. Commun*., **6**, 119 (2005).
2. W. Ho, J. C. Yu and J. Yu, *Langmuir*, **21**, 3486 (2005).
3. S. Kim, S. Hwang and W. Choi, *J. Phys. Chem. B*, **109**, 24260 (2005).
4. T. J. Kemp and R. A. McIntyre, *Polym. Degrad. Stabil*., **91**, 165 (2006).
5. I. Tseng, J. C. S. Wu and H. Chou, *J. Catal*., **221**, 432 (2004).
6. Z. Li, W. Shen, W. He and X. Zu, *J. Hazard. Mater*., **155**, 590 (2008).
7. R. Janes, L. J. Knightley and C. J. Harding, *Dyes Pigments*, **62**, 199 (2004).
8. H. J. Choi and M. Kang, *Int. J. Hydrogen Energ*., **32**, 3841 (2007).
9. M. Moore, *Environ. Int*., **32**, 967 (2006).
10. S. B. Lovern and R. Klaper, *Environ. Toxicol. Chem*., **25**, 1132 (2006).
11. C. G. Daughton, *Environ. Impact Asses. Rev*., **24**, 711 (2004).
12. A. N. Jha, *Mut. Res*., **552**, 1 (2004).
13. P. S. Huovinen, H. Penttila and M. R. Soimasuo, *Int. J. Circumpolar Health*, **59**, 15 (2000).
14. M. Tedetti and R. Sempere, *J. Photochem. Photobiol*., **82**, 389 (2006).
15. D. P. Hader and R. P. Sinha, *Mutat. Res*., **571**, 221 (2005).
16. J. F. Reeves, S. J. Davies, N. J. F. Dodd and A. N. Jha, *Mutat. Res*., **640**, 113 (2008).
17. S. Raisuddin and A. N. Jha, *Environ. Mol. Mutagen*., **44**, 83 (2004).
18. N. C. Bols, R. C. Ganassin, D. J. Tom and L. E. Lee, *Cytotechnology*, **16**, 159 (1994).
19. T. Uchino, H. Tokunaga, M. Ando and H. Utsumi, *Toxicol. Vitro*, **16**, 629 (2002).
20. R. Konaka, E. Kasahara, W. C. Dunlap, Y. Yamamoto, K. C. Chien and M. Inoue, *Redox Rep*., **6**, 319 (2001).
21. C. Chen, P. Lei, H. Ji, W. Ma, J. Zhao, H. Hidaka and N. Serpone, *Environ. Sci. Technol*., **38**, 329 (2004).
22. T. C. Long, N. Saleh, R. D. Tilton, G. V. Lowry and B. Veronesi, *Environ. Sci. Technol*., **40**, 4346 (2006).
23. C. Cox, *J. Pestic. Reform*., **11**, 2 (1991).
24. J. Gabbay, G. Borkow, J. Mishal, E. Magen, R. Zatcoff and Y. Shemer-Avni, *J. Ind. Text*., **35**, 323 (2006).
25. M. Heinlaan, A. Ivask, I. Blinova, H. C. Dubourguier and A. Kahru, *Chemosphere*, **71**, 1308 (2008).
26. M. Moore, *Environ. Int*., **32**, 967 (2006).
27. C. G. Daughton, *Environ. Impact Asses. Rev*., **24**, 711 (2004).
28. A. N. Jha, *Mut. Res*., **552**, 1 (2004).
29. M. K. Yeo and M. Kang, *Bull. Korean Chem. Soc*., **29**, 1179 (2008).
30. W. Kimmel, S. Ballard, B. K. Ullman and T. Schilling, *Dev. Dynam*., **203**, 253 (1995).
31. Z. Cao and Y. Li, *Biochem. Biophys. Res. Commun*., **292**, 50 (2002).
32. C. R. Wheeler, J. A. Salzman, N. M. Elsayed, S. T. Omaye and D. W. Korte, *Anal. Biochem*., **184**, 193 (1990).
33. W. H. Habig, M. J. Pabst and W. B. Jakoby, *J. Biol. Chem*., **249**, 7130 (1974).
34. C. M. Wood, *Target organ toxicity in marine and freshwater teleosts*, vol. I, Taylor & Francis, London (2001).
35. M. Grosell and C. M. Wood, *J. Exp. Biol*., **205**, 1179 (2002).
36. D. F. Alderdice, *Fish Physiol. Biochem*., **11A**, 163 (1988).
37. W. Möller, T. Hofer, A. Ziesenis and E. Karg, *J. Heyder. Toxicol. Appl. Pharm*., **182**, 197 (2002).
38. A. L. Lambert, J. B. Mangum, M. P. DELorme and J. I. Everitt, *Toxicol. Sci*., **72**, 339 (2003).
39. L. C. Renwick, K. Donaldson and A. *Clouter, Toxicol. Appl. Pharm*., **171**, 119 (2001).
40. R. Kohen and A. Nyska, *Toxicol. Pathol*., **6**, 620 (2002).
41. S. A. Kelly, C. M. Havrilla, T. C. Brady, K. H. Abramo and E. D. Levin, *Environ. Health Perspect*., **106**, 375 (1998).
42. L. E. Rikans and K. R. Hornbrook, *Biochem. Biophys. Acta*., **1362**, 116 (1997).
43. T. C. Long, N. Saleh, R. D. Tilton, G. V. Lowry and B. Veronesi, *Environ. Sci. Technol*., **40** , 4346 (2006).
44. P. C. Maness, S. Smolinski, D. M. Blake, Z. Huang, E. J. Wolfrum and W. A. Jacoby, *Appl. Environ. Microbiol*., **65**, 4094 (1999).
45. T. Ashikaga, M. Wada, H. Kobayashi, M. Mori, Y. Katsumura, H. Fukui, S. Kato, M. Yamaguchi and T. Takamatsu, *Mutat. Res-Gen. Tox. Ent*., **466**, 1 (2000).
46. T. Xia, M. Kovochich, J. Brant, M. Hotze, J. Sempf, T. Oberley, C. Sioutas, J. I. Yeh, M. R. Wiesner and A. E. Nel, *Nano Lett*., **6**, 1794 (2006).
47. M. G. Jonz and C. A. Nurse, *J. Comp. Neurol*., **497**, 817 (2006).